SEISMIC DESIGN AND STABILITY ASSESSMENT OF COMPOSITE FRAMING SYSTEMS

Jerome F. Hajjar[1)], Mark D. Denavit[2)], Tiziano Perea[3)], and Roberto T. Leon[4)]

1) Professor and Chair, Department of Civil and Environmental Engineering, Northeastern University, Boston, Massachusetts, USA
2) Graduate Research Assistant, Department of Civil and Environmental Engineering,
University of Illinois at Urbana-Champaign, Urbana, Illinois, USA
3) Associate Professor, Departamento de Materiales, Universidad Autónoma Metropolitana, Mexico DF, Mexico
4) Professor, Department of Civil and Environmental Engineering,
Virginia Polytechnic Institute and State University, Blacksburg, Virginia, USA
jf.hajjar@neu.edu, denavit2@illinois.edu, tperea@correo.azc.uam.mx, rleon@vt.edu

Abstract: This paper presents new strategies for the design of braced and unbraced frame structures that include concrete-filled steel tubes or steel reinforced concrete beam-columns as part of the seismic force resisting system. The paper first highlights experimental tests conducted on concrete-filled steel tube beam-columns subjected to cyclic biaxial bending plus axial compression. These tests provide new data for slender composite beam-columns that complement existing worldwide data. Corroborating analyses using a new mixed finite element beam formulation for composite members are presented. New approaches are then introduced for analysis and design of composite beam-columns, including determination of appropriate values of the flexural rigidities of composite beam-columns for use in second-order elastic analysis. The proposed stability assessment is based on Direct Analysis procedures, where member and frame stability are accounted for using reduced member rigidities and either directly modeling initial imperfections or including notional horizontal loads in lieu of calculating member effective length. Validation of these new approaches for design is made through comparison with worldwide experimental tests on composite members.

1. INTRODUCTION

Composite frames have been shown to be a sensible option for use as the primary lateral resistance system of building structures; and in many cases offers significant advantages over other lateral resistance systems (Hajjar 2002). However, there is a notable lack of quantitatively justified guidance for design of these structures. Specifically, little guidance is available regarding the value of stiffness that should be used in elastic analyses of composite frames, the recently developed direct analysis method for stability design of steel structures (AISC 2010) has not been validated for use with composite structures, and there is little data to justify the structural system response factors (i.e., R, C_d, and Ω_o) given in the specifications for seismic design of composite frames. This paper presents experimental and analytical work conducted as part of a NEES research project to build core knowledge on the behavior of composite columns and to develop rational design recommendations.

2. FULL SCALE SLENDER CFT BEAM-COLUMN EXPERIMENTS

2.1 Test Specimens

The specimens in the experimental program were selected to be both relatively slender in length and in width-to-thickness ratio. Few specimens with these attributes have been tested in prior research as noted in experimental databases (Leon et al. 2005, Goode and Lam 2011). In total, eighteen specimens were tested with variations in steel tube shape and size, length, and concrete strength (Table 1).

The tests were conducted at the Multi-Axial Sub-Assemblage Testing (MAST) facility at the University of Minnesota. The MAST system (Figures 1 and 2) consists of a stiff steel crosshead connected to 4 vertical actuators and 2 actuators in both horizontal directions, allowing 6 DOF control of the crosshead. Thick plates were welded to the ends of the specimens. The bottom plate rigidly connected the specimen to the strong floor and the top plate rigidly connected the specimen to the crosshead. Through control of crosshead different end conditions could be simulated, most often a fixed-free (K=2) condition was enforced.

The axially stiff yet flexurally compliant CFT beam-column specimens were a unique challenge to control. The axial strength of some of the specimens exceeded the vertical capacity of the system (5,900 kN) and the specimens retained strength at the lateral displacement capacity of the system (406 mm) although they were often being held in an unstable configuration by the crosshead. The specimens were subjected to a variety of successive load histories, providing a wealth of data useful for developing design recommendations and calibration of advanced nonlinear

computational models.

The first load case subjected the specimens to concentric axial load. Most specimens were held in a fixed-free (K=2) configuration [specimens 1-C5-18-5 and 18-C5-26-12 were held in a fixed-fixed (K=1) configuration]. Specifically, lateral forces and bending moments at the crosshead were force controlled to zero, while the specimen was loaded in axially in displacement control until the critical load was reached. The twist DOF was held in displacement control to zero due to the low torsional stiffness of the specimens.

Table 1   Test Matrix

Specimen	D or H	B	t	f'$_c$	F$_y$	L
	(mm)	(mm)	(mm)	(MPa)	(MPa)	(mm)
1-C5-18-5	141	---	3.15	37.9	383	5,499
2-C12-18-5	324	---	5.92	38.6	337	5,499
3-C20-18-5	508	---	5.92	40.0	328	5,525
4-Rw-18-5	508	305	7.39	40.7	365	5,537
5-Rs-18-5	508	305	7.39	40.7	365	5,537
6-C12-18-12	324	---	5.92	91.0	337	5,499
7-C20-18-12	508	---	5.92	91.0	328	5,534
8-Rw-18-12	508	305	7.39	91.7	365	5,553
9-Rs-18-12	508	305	7.39	91.7	365	5,553
10-C12-26-5	324	---	5.92	54.5	335	7,950
11-C20-26-5	508	---	5.92	55.8	305	7,995
12-Rw-26-5	508	305	7.39	56.5	406	7,957
13-Rs-26-5	508	305	7.39	57.2	383	7,969
14-C12-26-12	324	---	5.92	80.0	383	7,963
15-C20-26-12	508	---	5.92	80.0	293	7,976
16-Rw-26-12	508	305	7.39	80.7	381	7,957
17-Rs-26-12	508	305	7.39	80.7	380	7,963
18-C5-26-12	141	---	3.15	80.7	383	7,941

The second load case subjected the specimens to combined axial compression and uniaxial bending. This was achieved with vertical force control at a specified load and displacement control of the lateral DOFs. Again, most specimens were held in a fixed-free (K=2) configuration with bending moments at the crosshead were force controlled to zero [specimens 1-C5-18-5 and 18-C5-26-12 were held in a fixed-fixed (K=1) configuration]. The third load case maintained the same control as the second load case, but subjected the specimen to combined axial compression and biaxial bending.

Additional latter load cases were conducted, subjecting the specimens to torsion or alternate end conditions. Full details of the test program including these load cases and discussions on wet concrete effects are presented elsewhere (Perea 2010).
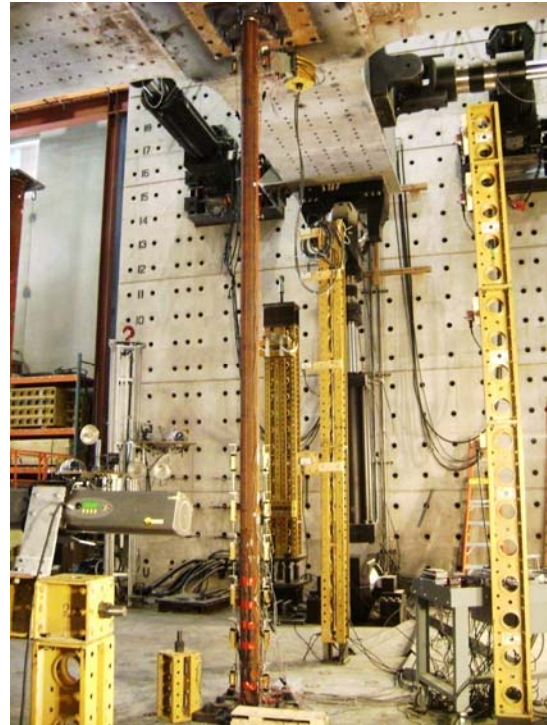

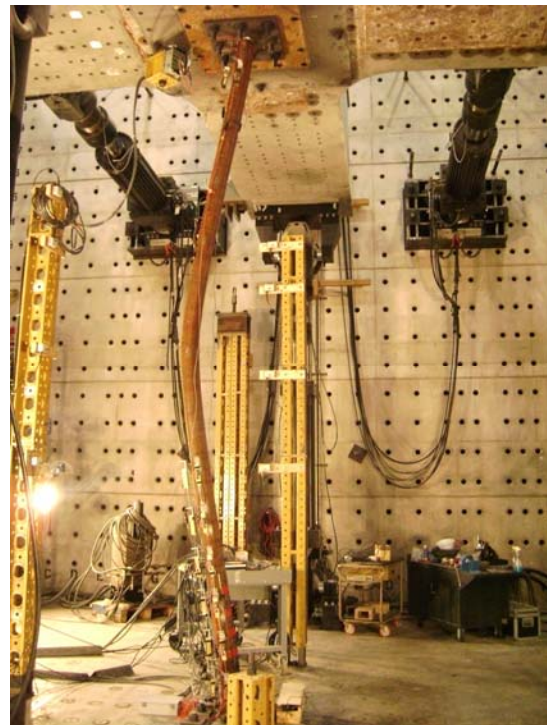
Figure 1   Specimen 1-C5-18-5 Before Testing

Figure 2   Specimen 1-C5-18-5 During Testing

2.2 Experimental Results

Typical results from load case 2 are shown in Figure 3. These results are from one axial load level, two cycles were performed. From these results, limit points (points on beam-column strength interaction surface) can be identified as the peak first order moment, or peak lateral load. It is noted that the second order moment continued to rise since the cross-section strength has not yet been reached and specimen was held in an unstable configuration by the displacement control of the crosshead. For each specimen, and each axial load level, a limit point was identified. The limit points for the specimens are presented in Figure 4 along with the design interaction diagram constructed using the plastic stress distribution method and points A, C, and B (AISC 2010). Since the ratio of axial load at point A (the pure axial strength) to the axial load at point C (a point axial load and moment equal to the pure bending strength) differs among the specimens, the range of interaction diagrams is shown with dashed lines and the average interaction diagram is shown as a solid line.
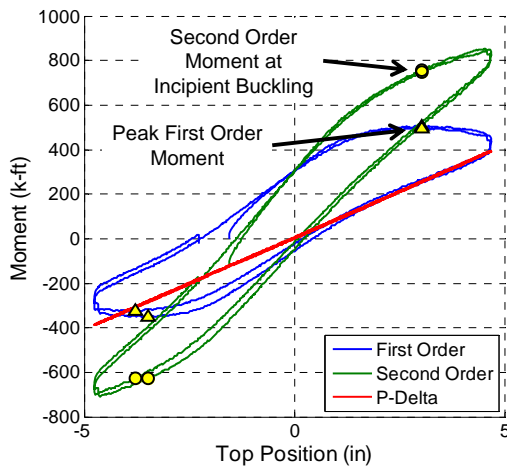

Figure 3   Determination of the Limit Point

The results of load case 2 also allow for an evaluation of the effective elastic stiffness (*EI*) of the composite section. The slope of force-deformation response (e.g., Figure 3) following load reversals was recorded (the very stiff response at the load reversal is attributed to friction in the loading system; care was taken to exclude these effects from the slope measurements). The recoded slope is then compared to an equivalent slope obtained from an elastic second-order analysis of a cantilever column with the same length and axial load. For each slope measured from the experimental data, a value of stiffness (*EI*) was determined such that the slope from the elastic analyses is equal to that from the experimental results. These results are normalized assuming that the contribution of the steel section is equal to its gross properties ($E_s I_s$) as described in Equation (1)

$$C = \left(EI_{measured} - E_s I_s \right) / E_c I_c \qquad (1)$$

The parameter can be regarded as the concrete contribution, a value of $C = 1$ would indicate that both the steel and concrete are contributing their full gross section properties to the flexural stiffness while a value of $C = 0$ would indicate that the concrete does not contribute at all to the flexural stiffness. The values of C obtained from load case 2 ranged from 0.30 to 0.45 with an average value of approximately 0.40 (Perea 2010).
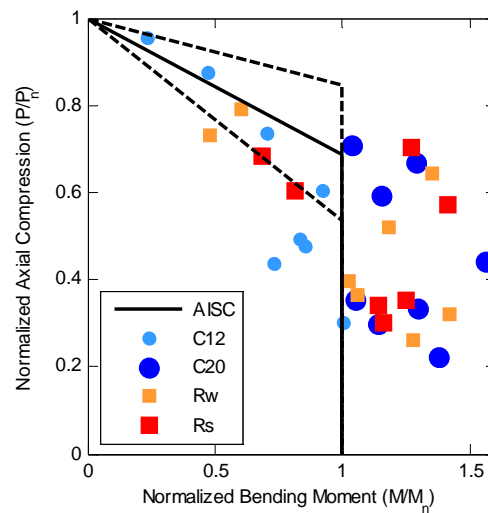

Figure 4   Second-Order Limit Points

3. MIXED FINITE ELEMENT MODELING OF COMPOSITE FRAME SYSTEMS

Frame analyses using distributed plasticity beam-column elements strike a favorable balance of computational efficiency and accuracy. Additionally, mixed formulations (defined here as treating both element displacements and stress resultants as primary state variables) allow for accurate modeling of both geometric and material nonlinearities. Tort and Hajjar (2010) developed a three-dimensional mixed beam element for the analysis of composite frames that include rectangular concrete-filled steel tube members, validating against a large number of experimental tests of composite members and frames. This finite element was adapted and further validated against an additional sets of experimental tests on circular concrete-filled steel tube members (Denavit and Hajjar 2012) and steel reinforced concrete members (Denavit et al. 2011).

The formulation relies on accurate constitutive relations to achieve accurate results. Numerous uniaxial constitutive relations have been proposed for composite members (e.g.,

El-Tawil and Deierlein 1999; Sakino et al. 2004). Typically, the relations are unique to the member type (i.e., SRC, RCFT, CCFT) because of differences in behavior, namely different confinement of the concrete, different residual stresses patterns, and different susceptibility to local buckling (which is often modeled as a material response). Different models use different assumptions and methods of calibration, but they generally strive to mimic the response of short concentrically loaded columns.

As part of the mixed beam formulation, a family of accurate uniaxial cyclic material models have been developed and reported by Tort and Hajjar (2007) for RCFTs, Denavit and Hajjar (2012) for CCFTs, and Denavit et al. (2011) for SRCs. The constitutive relation for the concrete core is adapted from the rule-based model of Chang and Mander (1994). The tensile branch and the cyclic rules were used without changes. However, the compressive branch was altered to reflect the state of confinement existing in the composite members. The steel model is based on the bounding-surface plasticity model of Shen et al. (1995). The model is used without modifications for the wide flange shapes within SRC sections; however, several modifications were made to model the behavior of the cold formed steel tubes in CFT sections. To model the built-in residual stress from cold-forming, an initial plastic strain is assumed. Local buckling is assumed to initiate when a certain critical strain has been reached. For compressive strains greater than the local buckling strain, the response is assumed to be a linear descending branch followed by a constant residual stress branch.

To validate the models, a large number of comparative analyses were performed (Tort and Hajjar 2007, Denavit and Hajjar 2012, Denavit et al. 2011). Sets of experimental data covering a wide variety of material properties, geometric properties, and loading configurations assembled. The slender beam-column tests described in this work were included in the validation study. Example results, comparing experimental and computational response of load cases 1 and 2 of specimen 11-C20-26-5, are shown in Figure 5.

4. STABILITY ANALYSIS AND DESIGN OF COMPOSITE FRAME SYSTEMS

The direct analysis method of stability design established within the AISC Specification for Structural Steel Buildings (AISC 2010) provides a straightforward and accurate way of addressing frame in-plane stability considerations (White et al. 2006). In this method, required strengths are determined with a second-order elastic analysis where members are modeled with a reduced stiffness and initial imperfections are either directly modeled or represented with notional lateral loads. The method allows for the computation of available strength based on the unsupported length of the column, eliminating the need to compute a K factor. The validity of this approach for steel structures has been established through comparisons between fully nonlinear analyses and elastic analyses

(Surovek-Maleck and White 2004). However, to date, no appropriate reduced elastic stiffness values have been developed nor has the methodology in general been validated for composite members.
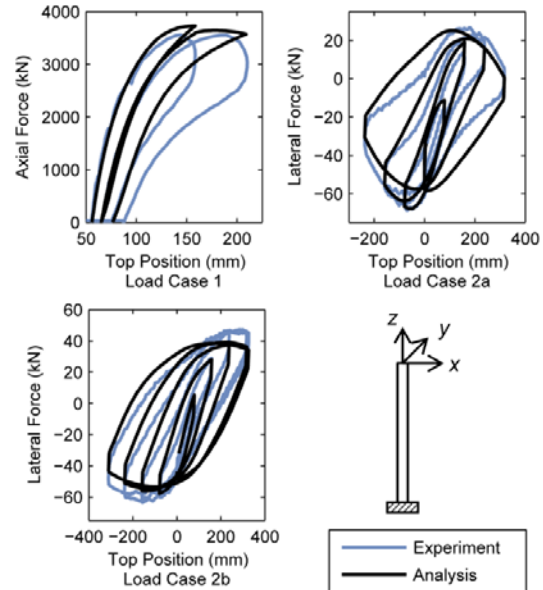

Figure 5   Validation Results (Specimen 11-C20-26-5)

In order to address these current needs in design, a large parametric study is being been conducted. The study focused on two related aspects of stability design. First is the development of an effective elastic stiffness, $EI_{elastic}$, for use in frame analyses with composite beam-columns. Second is the development and validation of Direct Analysis recommendations for strength design of composite systems as presented in detail in Denavit et al. (2012), the parametric study consists of comparisons between results from fully nonlinear analyses and elastic analyses on a set of benchmark frames. The fully nonlinear analyses are performed using the mixed beam finite element described above with the exception that simpler constitutive relations are selected to better correspond to assumptions common in the development of design recommendations.

The results of the study indicate that the Direct Analysis method can be extended to composite members with judicious selection of the elastic flexural stiffness and design interaction curve. One proposed option for the elastic flexural stiffness, $EI_{elastic}$, for CFT members is given in Equation (2) (Denavit et al. 2012). This value is subject to the stiffness reductions described within the Direct Analysis method.

$$EI_{elastic} = E_s I_s + 0.75 C_3 E_c I_c \qquad (2)$$

$$C_3 = 0.6 + 2\left(\frac{A_s}{A_s + A_c}\right) \le 0.9 \qquad (3)$$

The design interaction curve for a beam-column based on the plastic stress distribution method was shown to be suitable a majority of structures. This diagram is constructed with three anchor points: Point A, the pure axial strength; Point B, the pure bending strength; and Point C, a point axial load and moment equal to the pure bending strength (AISC 2010).

4.1 Experimental Validation of the Design Methodology

Since the design methodology was developed based on computational results, it is useful to validate the proposed recommendations against experimental data. The slender beam-column tests presented above are well suited for a comparison since second-order effects were significant and the specimens were well instrumented. Both strength and stiffness comparisons can be made using the results from load case 2.

The factor, $0.75C_3$, applied to the gross flexural stiffness of the concrete component in the elastic flexural stiffness expression given in Equation (2) is comparable to the factor, C, in Equation (1). The factor, $0.75C_3$, ranges from 0.52 to 0.58 for all of the slender beam-column specimens, where C_3 is computed with Equation (3). As stated above, the average value of C measured from load case 2 was 0.40. However, noting the significant scatter of the experimental results, the value proposed for design compares well to the experimental results.

Further comparisons are shown in Figures 6 through 9, where the limit points identified in load case 2 are plotted with interaction curves obtained using fully nonlinear analyses and the proposed design methodology for a subset of the specimens. The blue squares are the second-order internal forces at the limit point. Eight limit points were identified for each specimen in load case 2, one for each half cycle at each axial load level. The blue circles are the first-order applied forces at the limit point; the first-order moments are calculated as the product of the specimen length and the applied lateral load at the top of the beam-column.

The red interaction curves were developed using the same fully nonlinear model as employed to develop the design recommendations (Denavit et al. 2012) with the exception that measured initial out-of-plumbness was used in lieu of the nominal initial out-of-plumbness of L/500. A series of non-proportional analyses were performed at different axial load levels identifying the limit point as when the lowest Eigenvalue reached zero. The dashed curve represents the second-order internal forces and the solid curve represents the first-order applied forces.

The black dashed line is the design interaction curve constructed from Points A, C, and B (AISC 2010) with K=1 as specified in the Direct Analysis method. The black solid line is the first-order applied force interaction diagram. This curve is constructed by determining the applied loads that result in internal forces on the design interaction curve when modeled as prescribed by the Direct Analysis method (i.e., elastic second-order analysis, reduced elastic stiffness, and additive notional loads) with the exception that the notional loads were selected to represent the measured initial out-of-plumbness. The grey solid curve is the first-order applied force interaction diagram using nominal notional loads.

At both the second-order internal force level and the first-order applied force level, the fully nonlinear analysis and design methodology correspond well to the experimental results. The second-order internal forces are generally underestimated by the design interaction curve and better represented by the fully nonlinear analysis; this is due in part to the "bulge" in the interaction diagram near the balance point being neglected in the design interaction diagram.

The initial imperfections of the specimens are seen to have a significant effect at the first-order applied force level. The initial out-of-plumbness of specimen 8-Rw-18-5 (L/121) was greater than nominal, the effect of this can be seen in the lack of symmetry of the experimental and analytical results (Figure 8). The points that appear unconservative (i.e., blue circle inside the grey solid curve) are accurately captured when the notional load was adjusted to represent the measured imperfections, indicating that the lower strengths are primarily due to the greater than nominal initial imperfections.

5. CONCLUSIONS

Experimental and analytical work performed as part of a current NEES project has been presented. A series of full-scale slender beam-column tests were performed, subjecting CFTs to a wide range of loading. Axial compression-bending moment limit points and effective elastic stiffness were identified. A mixed beam finite element formulation specific to steel-concrete composite members was developed and utilized to develop stability design recommendations. One option for a proposed stability design methodology, developed in an ongoing study, was validated against the experimental results, indicating that safe and accurate results can be obtained using the Direct Analysis method with steel-concrete composite members.
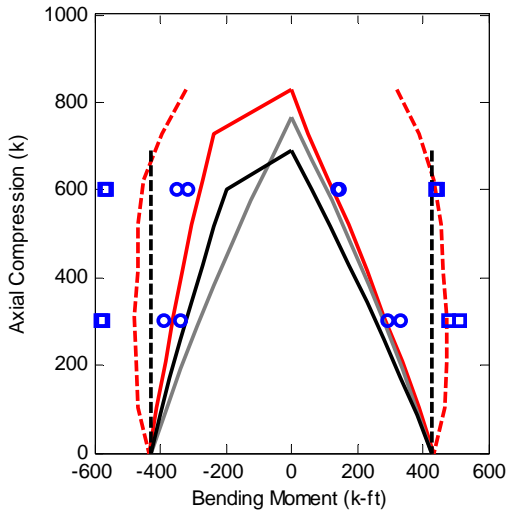
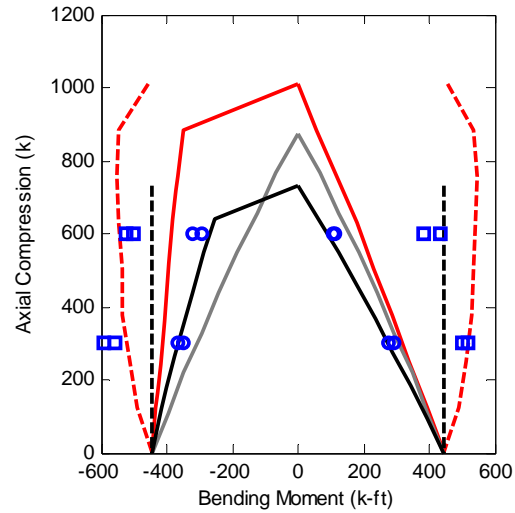Figure 6　Strength Comparisons (Specimen 4-Rw-18-5)

Figure 8　Strength Comparisons (Specimen 8-Rw-18-12)
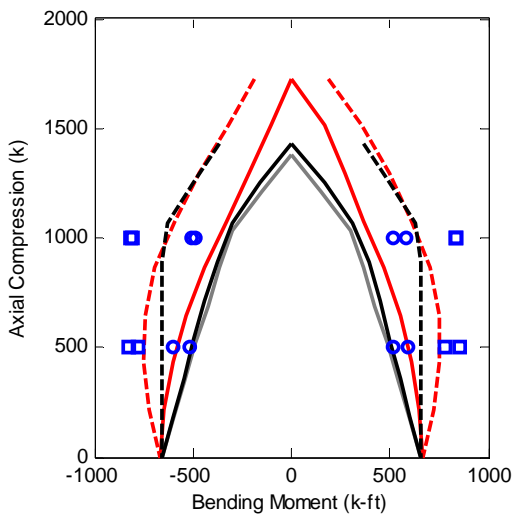

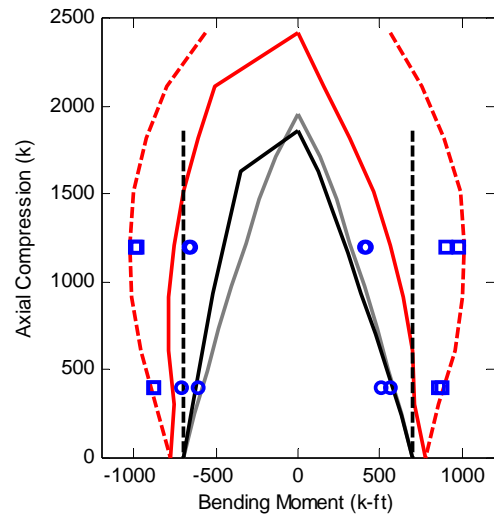Figure 7　Strength Comparisons (Specimen 5-Rs-18-5)

Figure 9　Strength Comparisons (Specimen 9-Rw-18-12)

References:

American Institute of Steel Construction (AISC) (2010). ANSI/AISC360-10: Specification for Structural Steel Buildings, AISC, Chicago, Illinois.

Chang, G. A., and Mander, J. B. (1994). Seismic Energy Based Fatigue Damage Analysis of Bridge Columns: Part I - Evaluation of Seismic Capacity. National Center for Earthquake Engineering Research, State University of New York at Buffalo, Department of Civil Engineering.

Denavit, M. D., Hajjar, J. F., and Leon, R. T. (2011). "Seismic Behavior of Steel Reinforced Concrete Beam-Columns and Frames," Proceedings of the ASCE/SEI Structures Congress 2011, Las Vegas, Nevada, April 14-16, 2011, ASCE, Reston, Virginia.

Denavit, M. D., Hajjar, J. F., and Leon, R. T. (2012). "Stability Analysis and Design of Steel-Concrete Composite Columns," Proceedings of the Annual Stability Conference, Structural Stability Research Council, Grapevine, Texas, April 18-21.

Denavit, M. D., and Hajjar, J. F. (2012). "Nonlinear Seismic Analysis of Circular Concrete-Filled Steel Tube Members and Frames." Journal of Structural Engineering, (in press).

El-Tawil, S., and Deierlein, G. G. (1999). "Strength and Ductility of Concrete Encased Composite Columns." Journal of Structural Engineering, 125(9), 1009-1019.

Goode, C. D. and Lam, D. (2011). "Concrete-Filled Steel Tube Columns – Test Compared with Eurocode 4", Composite Construction in Steel and Concrete VI (R. T. Leon et al., eds.) ASCE, Reston, pp. 317-325.

Hajjar, J. F. (2002). "Composite steel and concrete structural systems for seismic engineering," Journal of Constructional Steel Research, Vol. 58, No. 5-8, pp. 703-723.

Leon, R. T., Aho, M. F., and Kim, D. K. (2005). "A Database for Encased and Concrete-filled Columns," Internal Report, School of Civil and Environmental Engineering, Georgia Institute of Technology, Atlanta, GA.

Perea, T. (2010). "Analytical and Experimental Study on

Composite Concrete-Filled Steel Tube Beam-Columns," Ph.D. dissertation, School of Civil and Environmental Engineering, Georgia Institute of Technology, Atlanta, Georgia.

Sakino, K., Nakahara, H., Morino, S., and Nishiyama, I. (2004). "Behavior of Centrally Loaded Concrete-Filled Steel-Tube Short Columns," Journal of Structural Engineering, ASCE, Vol. 130, No. 2, pp. 180-188.

Shen, C., Mamaghani, I. H. P., Mizuno, E., and Usami, T. (1995). "Cyclic Behavior of Structural Steels. II: Theory." Journal of Engineering Mechanics, 121(11), 1165-1172.

Surovek-Maleck, A. E. and White, D. W. (2004). "Alternative Approaches for Elastic Analysis and Design of Steel Frames. II: Verification Studies," Journal of Structural Engineering, ASCE, Vo1. 30, No. 8, pp. 1197-1205.

Tort, C., and Hajjar, J. F. (2010). "Mixed Finite-Element Modeling of Rectangular Concrete-Filled Steel Tube Members and Frames under Static and Dynamic Loads." Journal of Structural Engineering, 136(6), 654-664.

White, D. W., Surovek, A. E., Alemdar, B. N., Chang, C. J., Kim, Y. D., and Kuchenbecker, G. H. (2006). "Stability Analysis and Design of Steel Building Frames Using the 2005 AISC Specification." Steel Structures, 6, 71-91.